GEOPHYSICS, VOL. 68, NO. 5 (SEPTEMBER-OCTOBER 2003); P. 1525–1536, 9 FIGS.
10.1190/1.1620626

An efficient finite-difference scheme for electromagnetic logging in 3D anisotropic inhomogeneous media

Sofia Davydycheva*, Vladimir Druskin‡, and Tarek Habashy‡

ABSTRACT

We consider a problem of computing the electromagnetic field in 3D anisotropic media for electromagnetic logging. The proposed finite-difference scheme for Maxwell equations has the following new features based on some recent and not so recent developments in numerical analysis: coercivity (i.e., the complete discrete analogy of all continuous equations in every grid cell, even for nondiagonal conductivity tensors), a special conductivity averaging that does not require the grid to be small compared to layering or fractures, and a spectrally optimal grid refinement minimizing the error at the receiver locations and optimizing the approximation of the boundary conditions at infinity. All of these features significantly reduce the grid size and accelerate the computation of electromagnetic logs in 3D geometries without sacrificing accuracy.

INTRODUCTION

In recent years and in connection with the development of horizontal and inclined drilling, it has become important to investigate anisotropic and highly-contrasted layered media intersected by a deviated borehole. We consider the problem of computing the electromagnetic fields in an inhomogeneous 3D anisotropic medium with anisotropy tensors whose principal axes are arbitrarily oriented in space. In more detail, geophysical motivation behind this problem and literature reviews on the petrophysics of electrically anisotropic rocks can be found in Anderson et al. (1999), Wang and Fang (2001), and Weiss and Newman (2002). In this paper, we concentrate on computational aspects of the forward modeling.

As a rule, problems of such type are usually solved by means of a finite-element (FE) method or a finite-difference (FD) method. The staggered grid modeling approach was proposed by Yee (1966) and, since that time, has been successfully applied to problems of computing electromagnetic fields in arbitrary 3D isotropic media by many authors [see Wang and Fang (2001) and Weiss and Newman (2002) for more detailed literature review]. This approach yields coercive approximation, that is, every continuous Maxwell equation has its discrete counterpart satisfying conservation laws (Gauss and Stokes theorems)—important features for a good approximation.

However, generalization of this approach to important practical 3D anisotropic models with arbitrary tensors of electric conductivity, magnetic permeability, and dielectric permittivity is not straightforward. Yee's (1966) scheme implies that different electric field components are defined at different points in space. This is enough for isotropic problems, where the constitutive relationships between vectors can be written independently for every component. For example, the isotropic Ohm's law connects only x-components of the electric field and the electric current, etc. However, in order to use Ohm's law with tensor conductivity (and similar constitutive laws with other anisotropy tensors), one needs to specify all three field components at every point to compute cross terms.

There are two main approaches to circumvent this difficulty enabling the implementation of anisotropy in Maxwell equations.

The first and more obvious approach is to interpolate the electric field from neighboring nodes (Weidelt, 1999; Wang and Fang, 2001; Weiss and Newman, 2002). This approach solves the problem in principle; however, the interpolation effectively doubles the size of the FD steps for the computation of the cross terms, so it brings additional errors.

Another important drawback of this interpolation approach is that, in contrary to the isotropic Yee scheme, not all the counterparts of the continuous anisotropic equations can be written in the local discrete form. For example, in the interpolation scheme, the electric current at a given node depends via the anisotropic Ohm's law only on the values of the electric field at the neighboring nodes. However, the inverse of a local interpolation operator cannot be local, so the inverse of the FD Ohm's law connects the electric field at one point

Manuscript received by the Editor April 23, 2002; revised manuscript received April 1, 2003.
*Schlumberger, Sugar Land Product Center, 110 Schlumberger Drive, MD5, Sugar Land, Texas 77478. E-mail: sdavydycheva@sugar-land.oilfield.slb.com.
‡Schlumberger-Doll Research, 36 Old Quarry Road, Ridgefield, Connecticutt 06877-4108. E-mail: vdruskin@ridgefield.oilfield.slb.com; thabashy@ridgefield.oilfield.slb.com.

with all the components of the electric current on the entire grid. Due to this phenomenon, for example, the second-order FD Maxwell system of Weiss and Newman (2002) cannot be equivalently rewritten in local form in terms of the magnetic field. Therefore, such an important physical principle as duality (symmetry) between electric and magnetic fields is lost in this FD implementation.

The above-mentioned phenomenon has been known from the 1960s, and one approach to overcome it is the so-called totally conservative (finite-volume) scheme suggested by Lebedev (1964). Such a scheme allows specifying all three components of the electric field at the same points on the grid without interpolation. This enables representing both Ohm's law and its inverse locally in the case of general anisotropy. Similarly to the isotropic Yee (1966) approximation, all the counterparts of the continuous relationships for the electromagnetic field exist in Lebedev's scheme. It is worth mentioning that the drawbacks of the interpolation approach were known in the geophysical literature (Igel et al., 1995), where Lebedev's scheme was independently proposed for anisotropic elasticity and then rejected because of an apparent fourfold increase of computational cost, a problem which is circumvented in this paper.

Lebedev's (1964) scheme was implemented for the solution of the Maxwell equation by Davydycheva and Druskin (1995, 1999). In the present paper, we report on the progress in this approach.

Lebedev's scheme can be split in four uncoupled (primary and dual) conventional staggered schemes. As it was correctly noticed by Igel et al. (1995), Wang and Fang (2001), and Weiss and Newman (2002), such a splitting can increase computational cost fourfold compared to the standard Yee grid in isotropic media. To circumvent this problem, we modify the condition at the external boundary of computational domain and the summation of the total solution. As a result, we are able to take advantage of the error cancellation properties of the primary and dual schemes, so even for homogeneous isotropic medium our scheme becomes more efficient than the standard Yee grid.

Even for the case of an isotropic medium, contrast discontinuities can often introduce gross errors within the standard FD approach if not properly handled, unless the interfaces are gridded in detail, which may require unrealistically large-size grids. Of course, introducing fine dipping layers with crossbedding or nonconformal thin fractures would make accurate approximation of Maxwell equation even more challenging. To circumvent this problem, we use the equivalent medium approach of Moskow et al. (1999) that allows homogenization of the medium enclosed inside a grid cell. The advantage of this approach is that it allows constructing the grid independently of the medium model.

In the induction logging problem, it is assumed that the sources and receivers are located at the borehole axis. Typically one needs to compute the electromagnetic fields only along that line and is not so interested in accurate solutions elsewhere. It is well known that the grid should be refined towards the source-receiver locations, but until recently it was not known how to optimize such refinements (at least for the FD). It was shown by Druskin and Knizhnerman (1999) that a proper grid refinement (so-called "optimal" grids) can make second-order FD schemes exponentially convergent. Such grids are obtained by minimizing the FD impedance error at the receiver, as opposed to the standard adaptive grids that minimize the global truncation error. The optimal grids use only generic asymptotic spectral properties of the Green's functions and, in many cases (such as in induction logging where typically skin depth is much larger than the minimal FD grid steps), can be done a priori independently of the conductivity model. Another important feature of such grids is that they are constructed based on the same rational approximation principles as the absorbing boundary conditions for wave equations, so they produce an optimal domain truncation. Applied to hyperbolic problems the optimal grid approach has shown about one order acceleration for typical 2.5D acoustic logging problems (Asvadurov et al., 2000). In this paper, we accelerate the computation of the dissipative electromagnetic problem at hand using optimal geometric grids developed by Ingerman et al. (2000).

We successfully implemented the new scheme within the framework of the spectral Lanczos decomposition method (SLDM) (Druskin and Knizhnerman, 1994) for high-frequency problems and its preconditioned modification (Druskin et al., 1999) for low frequencies. However, we believe that, due to a small grid size of our optimized FD approximation, direct solvers potentially can be more efficient.

GRID DISCRETIZATION OF MAXWELL EQUATIONS

Consider the frequency-domain Maxwell equations with anisotropic coefficients in 3D space $\mathbf{R}^3$;

$$\nabla \times \mathbf{E} = \mathrm{i}\omega\boldsymbol{\mu}\mathbf{H}, \quad \nabla \times \mathbf{H} = \boldsymbol{\sigma}\mathbf{E} - \mathrm{i}\omega\boldsymbol{\varepsilon}\mathbf{E} + \mathbf{J}, \qquad (1)$$

with zero boundary conditions at infinity. Here $\mathbf{E} \equiv (E_x, E_y, E_z)$ and $\mathbf{H} \equiv (H_x, H_y, H_z)$ are the electric and magnetic field vectors, respectively, and $\mathbf{J} \equiv (J_x, J_y, J_z)$ is the transmitter current density, with the time dependence $\exp(-\mathrm{i}\omega t)$ assumed. The conductivity $\sigma(x, y, z)$, magnetic permeability $\mu(x, y, z)$, and dielectric permittivity $\varepsilon(x, y, z)$ are symmetric nonnegative definite 3×3 tensors.

Introduce a Cartesian 3D grid,

$$(x_i, y_j, z_k), \quad i = 0, 1, \ldots, M_x;$$
$$j = 0, 1, \ldots, M_y; \quad k = 0, 1, \ldots, M_z, \qquad (2)$$

where M_x, M_y, and M_z are even numbers. Denote subgrids P and R as follows: let the subgrid P contain nodes with even sum of indices (three even numbers or one even number and two odd ones), whereas the subgrid R contains the rest of the grid. Denote functions with upper indices P or R as approximations on the corresponding subgrid.

We substitute the unbounded medium $\mathbf{R}^3$ by the rectangular computational domain $\Omega = [x_0, x_{M_x}] \times [y_0, y_{M_y}] \times [z_0, x_{M_z}]$. Obviously, its boundary $\partial\Omega$ contains nodes of both subgrids P and R.

Define finite differences along the x axis,

$$f_x^P = \left\{\left(f_x^P\right)_{i,j,k}\right\}, \quad \left(f_x^P\right)_{i,j,k} = \frac{{f^R}_{i+1,j,k} - {f^R}_{i-1,j,k}}{x_{i+1} - x_{i-1}},$$

$$f_x^R = \left\{\left(f_x^R\right)_{i,j,k}\right\}, \quad \left(f_x^R\right)_{i,j,k} = \frac{{f^P}_{i+1,j,k} - {f^P}_{i-1,j,k}}{x_{i+1} - x_{i-1}}, \qquad (3)$$

and similarly along the y and z axes. Obviously, finite differences defined in this way perform mapping from P to R and vice versa, because $(i, j, k) \in P \Leftrightarrow (i \pm 1, j, k) \in R$. Therefore, if we consider the grid approximation of the electric field $\mathbf{E}^R$ on the subgrid R, the approximations of the magnetic field obtained by using the grid curl of $\mathbf{E}^R$ will be defined on the subgrid P.

Thus, we can write a grid approximation of Maxwell equations following equations (1):

$$\tilde{\nabla} \times \mathbf{E}^R = \mathrm{i}\omega\boldsymbol{\mu}^P\mathbf{H}^P,$$
$$\tilde{\nabla} \times \mathbf{H}^P = \boldsymbol{\sigma}^R\mathbf{E}^R - \mathrm{i}\omega\boldsymbol{\varepsilon}^R\mathbf{E}^R + \mathbf{J}^R, \qquad (4)$$

where $\tilde{\nabla}\times$ is the grid curl defined using equation (3). In this way, a system for $\mathbf{E}^R$ can be derived:

$$\tilde{\nabla} \times [(\boldsymbol{\mu}^P)^{-1}\tilde{\nabla} \times \mathbf{E}^R] - \mathrm{i}\omega\dot{\boldsymbol{\sigma}}^R\mathbf{E}^R = \mathrm{i}\omega\mathbf{J}^R, \qquad (5)$$

where $\dot{\boldsymbol{\sigma}}^R = \boldsymbol{\sigma}^R + \mathrm{i}\omega\boldsymbol{\varepsilon}^R$. Similarly, the equivalent dual system for $\mathbf{H}^P$ can be written as

$$\tilde{\nabla} \times [(\dot{\boldsymbol{\sigma}}^R)^{-1}\tilde{\nabla} \times \mathbf{H}^P] - \mathrm{i}\omega\boldsymbol{\mu}^P\mathbf{H}^P = \mathrm{i}\omega\tilde{\nabla} \times (\dot{\boldsymbol{\sigma}}^R)^{-1}\mathbf{J}^R.$$

The zero boundary conditions at infinity can be replaced by the conditions

$$\mathbf{E}^R|_{\partial\Omega} \times \mathbf{n} = 0, \quad \mathbf{H}^P|_{\partial\Omega} \times \mathbf{n} = 0, \qquad (6)$$

where $\mathbf{n}$ is the vector normal to $\partial\Omega$.

As we mentioned in the Introduction, the existence of the equivalent dual FD system is one of the advantages of Lebedev's (1964) approach. It insures that $\mathbf{H}^P$ can be accurately computed from $\mathbf{E}^R$ and vice versa. We should point out that in the already mentioned interpolation approach (Weidelt, 1999; Wang and Fang, 2001; Weiss and Newman, 2002), the dual system for magnetic fields can not be written in a local FD form because of the nonlocality of the inverse of the interpolation operator.

Connection with the standard Yee scheme

Consider a group of elements of the subgrid functions $\mathbf{E}^R$ and $\mathbf{H}^P$ with the following indices:

$$E_x^R(1,0,0), \quad E_y^R(0,1,0), \quad E_z^R(0,0,1),$$
$$H_x^P(0,1,1), \quad H_y^P(1,0,1), \quad H_z^P(1,1,0),$$

where, for brevity, (1,0,0) denotes $(2i+1, 2j, 2k)$, (0,1,0) denotes $(2i, 2j+1, 2k)$, etc. It can be shown that they are nothing but the elements of the standard Yee scheme for the isotropic problem (Druskin and Knizhnerman, 1994; Yee, 1966). This group is called cluster 000 (see Figure 1).

Now consider the elements of the same components $\mathbf{E}^R$ and $\mathbf{H}^P$ with shifted indices:

$$E_x^R(0,0,1), \quad E_y^R(1,1,1), \quad E_z^R(1,0,0),$$
$$H_x^P(1,1,0), \quad H_y^P(0,0,0), \quad H_z^P(0,1,1).$$

We denote this group as cluster 101. Then, let clusters 110 and 011 be, respectively,

$$E_x^R(0,1,0), \quad E_y^R(1,0,0), \quad E_z^R(1,1,1),$$
$$H_x^P(1,0,1), \quad H_y^P(0,1,1), \quad H_z^P(0,0,0);$$

$$E_x^R(1,1,1), \quad E_y^R(0,0,1), \quad E_z^R(0,1,0),$$
$$H_x^P(0,0,0), \quad H_y^P(1,1,0), \quad H_z^P(1,0,1).$$

One can easily show that the finite-difference operator $\tilde{\nabla}\times$ defined by formulas (3) performs mapping within each cluster independently. Coupling between clusters in equation (5) is performed by nondiagonal elements of the matrices $\boldsymbol{\sigma}^R, \boldsymbol{\mu}^P, \boldsymbol{\varepsilon}^R$ only. They relate elements defined at the same node of the grid but belonging to different clusters, as it is shown in Figure 1 for the components of the electric field. It is easy to see that the components E_x^R and E_z^R belonging to different clusters are defined at the same nodes. If the matrices $\boldsymbol{\sigma}^R, \boldsymbol{\mu}^P, \boldsymbol{\varepsilon}^R$ are diagonal (isotropic case), equation (5) can be divided into four uncoupled clusters. Each of these clusters coincides with the standard Yee system.

Averaging of sources, solutions, and error cancellation

The discrete source has to be properly introduced for every cluster, otherwise the solution on some clusters can be identically zero. We obtain the electromagnetic field as a linear combination of the solution on the four clusters with properly chosen weights. As we will see, such a "proper" averaging greatly reduces the approximation error compared to a single Yee grid.

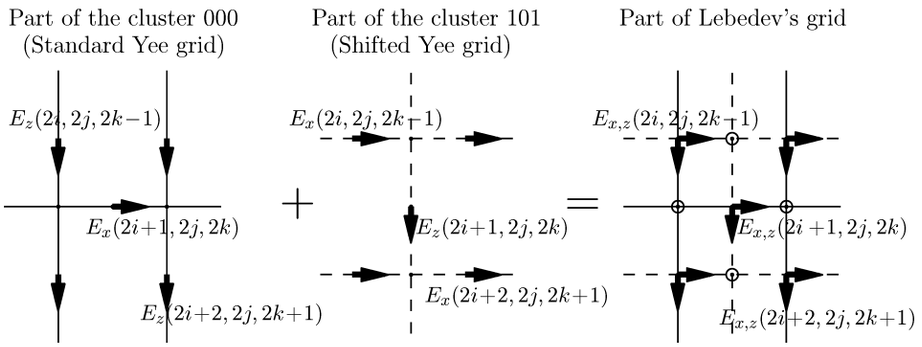

FIG. 1. Two-dimensional cross-section (in the plane Oxz) of Lebedev's staggered grid consisting of two clusters. The thick double arrows in the right diagram denote the subgrid R ("electric" nodes) of Lebedev's grid, whereas the nodes of the subgrid P ("magnetic" ones) are denoted by circles. The magnetic nodes are located in staggered order with respect to the "electric" nodes.

Let us consider for simplicity the problem of computation of the Green's function of a unit electric x-oriented source dipole located at a point $(x_{i_0}, y_{j_0}, z_{k_0})$. Let, for example, this point be at cluster (000), then the point with indices $(i_0+1,\ j_0+1,\ k_0)$ be at (110), etc. We place sources (x-oriented dipoles) at $(i_0,\ j_0, k_0)$ and at some four points for each of the remaining three clusters. These twelve points have indices $(i_0+\ell_x,\ j_0+\ell_y, k_0+\ell_z$, where the shifts ℓ_x, ℓ_y, ℓ_z are given by all combinations of ± 1 and 0 satisfying the condition

$$|\ell_x| + |\ell_y| + |\ell_z| = 2. \tag{7}$$

The weights (strengths of the sources) are defined by the following two conditions: (1) the sum of the sources in every cluster must be equal to 1; (2) the center of the mass of the source distribution in every cluster should be located at $(x_{i_0}, y_{j_0}, z_{k_0})$.

Suppose we want to compute a component of the electric field at a point $(x_{i_0}, y_{j_0}, z_{k_0})$. Let, for simplicity, that point again belongs to (000). Then, on this cluster we just take the solution at $(x_{i_0}, y_{j_0}, z_{k_0})$. Solutions on each of the remaining clusters should be obtained by linear interpolation from the nearest points [i.e., $(x_{i_1+\ell_x}, y_{j_1+\ell_y}, z_{k_0+\ell_z})$ with the shifts satisfying condition (7)]. The final solution is the arithmetic average of the solutions on the four clusters.

We will see that even for isotropic media the above averaging procedure together with the boundary condition (6) increases drastically the accuracy of the total solution compared to the one computed on each cluster separately.

In Figures 2 and 3, we show the magnetic induction B_x of a x-oriented magnetic dipole (B_{xx}) computed in a homogeneous whole space. We compare the analytic solution with the ones obtained using Yee and Lebedev's grids. The Yee grid (basic cluster with the "electric" boundary condition) corresponds to the cluster (000), under the compensating clusters we mean the remaining three clusters. As we see, the compensation drastically increase accuracy compared to the single Yee grid. At least in the case of the homogeneous isotropic medium, the presented results coincide rather precisely with the analytical solution everywhere, whereas this is impossible when using the standard Yee grid. Especially remarkable is that Lebedev's grid yields an accurate approximation starting from the nodes immediately adjacent to the transmitter and the outer boundary, as is shown in Figures 2 and 3, respectively. We will rigorously explain this phenomenon in a following sections.

Let us note that Davydycheva and Druskin (1995, 1999) used another way to approximate the field in the vicinity of the transmitter and at the outer boundary. The grid dipole moments of the transmitter in that work were taken to be equal on different clusters, and Davydycheva and Druskin implemented only electric boundary conditions at the boundary of the domain. Thus, in the case of isotropic models, they got four identical independent sets of the equations, each of them coinciding with the standard Yee scheme. Since the results on the different clusters were also identical, three of them were redundant. In our new approach, we force the clusters to cancel the errors of each other.

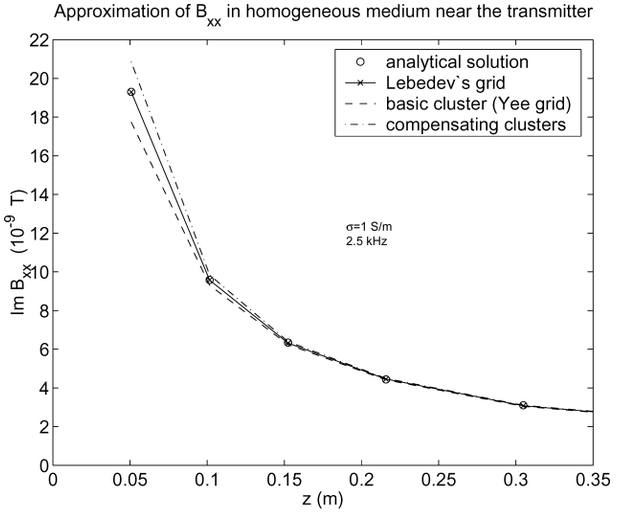

FIG. 2. Cancellation of the errors of $\mathrm{Im}B_{xx}$ in the vicinity of the transmitter due to properly chosen grid source currents on different clusters. The field computed on Lebedev's grid and separately on different clusters is depicted. The clusters effectively compensate each other, or cancel the errors, after averaging the field over them.

GRID COEFFICIENTS APPROXIMATION

Important to such an approach is the development of a material averaging formula that gives an effective medium corresponding to a heterogeneously varying conductivity enclosed within the grid cells.

Let us consider the grid approximation of the conductivity $\boldsymbol{\sigma}^R$. Consider a finely layered, transversely homogeneous medium stratified along an arbitrary N-direction. We use two different schemes for obtaining the averaging formulas. The first one we call standard homogenization, since it corresponds to the addition rules of resistances and conductances in electric circuits.

In the case when the layers are isotopic, it is easy to show that these rules yield the averaged tensor $\boldsymbol{\Sigma}$ with the following normal ($\boldsymbol{\Sigma}_{NN}$), transverse ($\boldsymbol{\Sigma}_{TT}$), and nondiagonal components

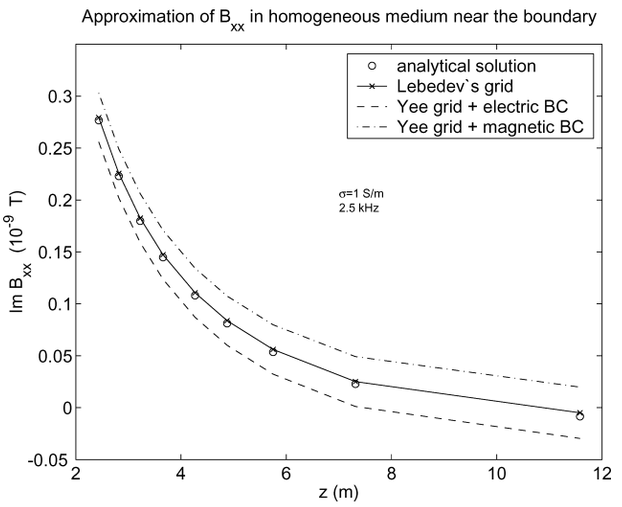

FIG. 3. Cancellation of the errors of $\mathrm{Im}B_{xx}$ at the outer boundary due to the combined boundary conditions. The errors induced by truncating the domain have opposite signs on different clusters, depending on the boundary conditions, so the errors are cancelled after summing the field over the clusters.

($\boldsymbol{\Sigma}_{TN}$ and $\boldsymbol{\Sigma}_{NT}$):

$$\boldsymbol{\Sigma}_{NN} = \left\langle (\boldsymbol{\sigma}^R)^{-1} \right\rangle^{-1}, \quad \boldsymbol{\Sigma}_{TT} = \left\langle \boldsymbol{\sigma}^R \right\rangle,$$
$$\boldsymbol{\Sigma}_{TN} = 0, \quad \boldsymbol{\Sigma}_{NT} = 0, \tag{8}$$

where $< \cdots >$ refers to a spatial (volumetric) averaging.

The second scheme we call nodal homogenization. It is based on the rule that the energy within each grid cell is unchanged after averaging. That is, the integral of the current density multiplied by the electric field over the grid cell is the same for the initial and the effective media. This scheme is described in detail by Moskow et al. (1999).

Both averaging schemes were investigated by Moskow et al. (1999), where a similar problem for the dc-case was considered. It was shown that standard averaging works well enough to compute the electric field in the presence of thin-contrast highly resistive or conductive inclined structures, but that nodal averaging works even better, especially for high-resistive thin structures. Neither approach requires the grid to be small with respect to the thickness of individual layers. For example, it was shown that even for a contrast as high as 1:500 and for a thickness as small as one-fifth of the grid size, the relative error of the electric field computed outside the inhomogeneity does not exceed a few percent. This is despite the fact that the FD scheme implies that the electric field is constant within every grid cell, whereas in reality its normal component has a jump of 500 times across the contrast.

The examples shown in this paper are adequately modeled using the standard homogenization approach. For this reason and for the benefit of completeness, we derive in this section the standard averaging formula for an arbitrary anisotropic media, based on a paper by Habashy et al. (1993).

Let us assume that each layer is a general anisotropic homogeneous medium, whose conductivity is an arbitrary tensor $\boldsymbol{\sigma}$. Suppose that the layers extend infinitely along both transverse directions, and their thicknesses are much smaller than the skin depth at the frequency of the exciting electromagnetic field.

The constitutive relation of each layer is given by

$$\mathbf{J} = \boldsymbol{\sigma} \cdot \mathbf{E}.$$

Since the layer thickness is much shorter than the skin depth, the electric field $\mathbf{E}$ as well as the current $\mathbf{J}$ are almost uniform within each layer. From the boundary conditions (viz., the continuity of the transverse components of the electric field $\mathbf{E}_T$ and the normal component of the current J_N at the boundaries separating the layers), we deduce that $\mathbf{E}_T$ and J_N will only vary very slowly over the composite of the fine layers. On the other hand, the transverse components of the current $\mathbf{J}_T$ and the normal component of the electric field E_N will vary rapidly from layer to layer due to the variation in the conductivities of the layers.

From the above discussion, we can cast the constitutive relation in the following form:

$$\mathbf{J} = \begin{bmatrix} \mathbf{J}_T \\ J_N \end{bmatrix} = \begin{bmatrix} \boldsymbol{\sigma}_{TT} & \boldsymbol{\sigma}_{TN} \\ \boldsymbol{\sigma}_{NT} & \boldsymbol{\sigma}_{NN} \end{bmatrix} \cdot \begin{bmatrix} \mathbf{E}_T \\ E_N \end{bmatrix}.$$

Employing this representation, we express the rapidly varying transverse components of the current $\mathbf{J}_T$ and the normal component of the electric field E_N in terms of the slowly varying transverse components of the electric field $\mathbf{E}_T$ and the normal component of the current J_N to obtain

$$E_N = \boldsymbol{\sigma}_{NN}^{-1} \cdot J_N - \boldsymbol{\sigma}_{NN}^{-1} \cdot \boldsymbol{\sigma}_{NT} \cdot \mathbf{E}_T,$$
$$\mathbf{J}_T = \boldsymbol{\sigma}_{TN} \cdot \boldsymbol{\sigma}_{NN}^{-1} \cdot J_N + \left(\boldsymbol{\sigma}_{TT} - \boldsymbol{\sigma}_{TN} \cdot \boldsymbol{\sigma}_{NN}^{-1} \cdot \boldsymbol{\sigma}_{NT}\right) \cdot \mathbf{E}_T.$$

Upon averaging, we obtain

$$\langle E_N \rangle = \langle \boldsymbol{\sigma}_{NN}^{-1} \rangle \cdot J_N - \left\langle \boldsymbol{\sigma}_{NN}^{-1} \cdot \boldsymbol{\sigma}_{NT} \right\rangle \cdot \mathbf{E}_T,$$
$$\langle \mathbf{J}_T \rangle = \left\langle \boldsymbol{\sigma}_{TN} \cdot \boldsymbol{\sigma}_{NN}^{-1} \right\rangle \cdot J_N + \left(\langle \boldsymbol{\sigma}_{TT} \rangle - \left\langle \boldsymbol{\sigma}_{TN} \cdot \boldsymbol{\sigma}_{NN}^{-1} \cdot \boldsymbol{\sigma}_{NT} \right\rangle \right) \cdot \mathbf{E}_T.$$

Finally, to obtain the conductivity of the averaged medium, we express the averaged current in terms of the averaged electric field:

$$J_N = \left\langle \boldsymbol{\sigma}_{NN}^{-1} \right\rangle^{-1} \cdot \langle E_N \rangle + \left\langle \boldsymbol{\sigma}_{NN}^{-1} \right\rangle^{-1} \cdot \left\langle \boldsymbol{\sigma}_{NN}^{-1} \cdot \boldsymbol{\sigma}_{NT} \right\rangle \cdot \mathbf{E}_T,$$
$$\langle \mathbf{J}_T \rangle = \left\langle \boldsymbol{\sigma}_{TN} \cdot \boldsymbol{\sigma}_{NN}^{-1} \right\rangle \cdot \left\langle \boldsymbol{\sigma}_{NN}^{-1} \right\rangle^{-1} \cdot E_N + \left(\langle \boldsymbol{\sigma}_{TT} \rangle - \left\langle \boldsymbol{\sigma}_{TN} \cdot \boldsymbol{\sigma}_{NN}^{-1} \cdot \boldsymbol{\sigma}_{NT} \right\rangle + \left\langle \boldsymbol{\sigma}_{TN} \cdot \boldsymbol{\sigma}_{NN}^{-1} \right\rangle \cdot \left\langle \boldsymbol{\sigma}_{NN}^{-1} \right\rangle^{-1} \cdot \left\langle \boldsymbol{\sigma}_{NN}^{-1} \cdot \boldsymbol{\sigma}_{NT} \right\rangle \right) \cdot \mathbf{E}_T.$$

Hence, the constitutive relation for the averaged medium is represented by

$$\langle \mathbf{J} \rangle = \boldsymbol{\Sigma} \cdot \langle \mathbf{E} \rangle,$$

or

$$\begin{bmatrix} \langle \mathbf{J}_T \rangle \\ J_N \end{bmatrix} = \begin{bmatrix} \boldsymbol{\Sigma}_{TT} & \boldsymbol{\Sigma}_{TN} \\ \boldsymbol{\Sigma}_{NT} & \boldsymbol{\Sigma}_{NN} \end{bmatrix} \cdot \begin{bmatrix} \mathbf{E}_T \\ \langle E_N \rangle \end{bmatrix}$$

where

$$\boldsymbol{\Sigma}_{TT} = \langle \boldsymbol{\sigma}_{TT} \rangle - \left\langle \boldsymbol{\sigma}_{TN} \cdot \boldsymbol{\sigma}_{NN}^{-1} \cdot \boldsymbol{\sigma}_{NT} \right\rangle + \left\langle \boldsymbol{\sigma}_{TN} \cdot \boldsymbol{\sigma}_{NN}^{-1} \right\rangle \cdot \left\langle \boldsymbol{\sigma}_{NN}^{-1} \right\rangle^{-1} \cdot \left\langle \boldsymbol{\sigma}_{NN}^{-1} \cdot \boldsymbol{\sigma}_{NT} \right\rangle,$$
$$\boldsymbol{\Sigma}_{TN} = \left\langle \boldsymbol{\sigma}_{TN} \cdot \boldsymbol{\sigma}_{NN}^{-1} \right\rangle \cdot \left\langle \boldsymbol{\sigma}_{NN}^{-1} \right\rangle^{-1},$$
$$\boldsymbol{\Sigma}_{NT} = \left\langle \boldsymbol{\sigma}_{NN}^{-1} \right\rangle^{-1} \cdot \left\langle \boldsymbol{\sigma}_{NN}^{-1} \cdot \boldsymbol{\sigma}_{NT} \right\rangle,$$
$$\boldsymbol{\Sigma}_{NN} = \left\langle \boldsymbol{\sigma}_{NN}^{-1} \right\rangle^{-1}. \tag{9}$$

This derivation assumes that the finely layered composite can be represented by an effective averaged medium. When the conductivity inside of a grid cell is an arbitrary 3D function, we choose as the effective direction of layering that of maximum variation of the conductivity. We construct such a direction ($\hat{\mathbf{m}}$) so that $\nabla \cdot [\boldsymbol{\sigma}(\mathbf{r}) \cdot \hat{\mathbf{m}}] = 0$ in a least-squares sense by minimizing the functional

$$\int_\Omega d\mathbf{r} \{\nabla \cdot [\boldsymbol{\sigma}(\mathbf{r}) \cdot \hat{\mathbf{m}}]\}^2, \quad \text{subject to} \|\hat{\mathbf{m}}\| = 1. \tag{10}$$

However, for the models of the medium considered below, the direction of layering is obvious for most of the grid cells: it is the direction perpendicular to the border of the borehole, invasions, or layers, depending on the cell's position.

OPTIMAL GRID APPROACH

Above, we presented a general scheme to calculate the electromagnetic field of an arbitrary configuration of the transmitters, at any point of the space.

However, for a very important special case, when the transmitters and receivers are placed along one line (usually this is the z-axis which coincides with the axis of the borehole; however, an eccentric borehole is also possible), the grid size can be drastically reduced without loss of accuracy. This can be achieved by using the asymptotically-optimal grids outside the region where the transmitters and the receivers are situated (i.e., along the x- and y-axes). The concept of optimal grids was recently introduced by Druskin and Knizhnerman (1999, 2000). Since then it has been successfully applied to a number of problems, including such complicated ones as the solution of acoustic logging problems in elastic media (Asvadurov et al., 2000, 2002). It is known that for standard equidistant grids, the FD error is controlled by the grid step and the distance to boundary of the computational domain. Obviously, a nonuniform grid with the same minimal step and boundary of the computational domain would require much fewer steps than the equidistant grid. However, too rapid "coarsening" can significantly increase the error. The optimal grids provide a maximally possible grid nonuniformity without introducing significant additional errors. The optimal gridding can be considered to be an extension of the concept of the Gaussian quadrature rule for numerical integration to finite differences. The basic concept of the optimal grid was developed for the standard staggered FD scheme (i.e., the Yee scheme). However, as we recently found, for Lebedev's grid an even stronger result can be obtained. We start with the description of the optimal grid for a single Yee grid (cluster), and then show how the convergence rate can be improved for Lebedev's grid.

Background of the theory of optimal grids

Here, we briefly outline the concept of the optimal grids according to works by Druskin and Knizhnerman (1999, 2000) and Ingerman et al. (2000). First, as the simplest illustration, we consider the approximation of the electromagnetic field of the electric dipole (dc case) in 2D space $\mathbf{R}^2$ and discuss the extension to induction problems later. Let us assume that the z-oriented electric dipole (of strength 2) is located at the origin of the plane Oxz, and we need to compute the electric potential only along the line $x=0$ that corresponds to the measurements at the borehole axis. The electric potential satisfies Poisson equation,

$$-\frac{\partial^2 w(x,z)}{\partial z^2}-\frac{\partial^2 w(x,z)}{\partial x^2}=2\delta(x)\frac{d\delta(z)}{dz}, \tag{11}$$

and zero condition at infinity.

For simplicity, we analyze only the FD approximation along x, assuming that the approximation along z is exact. However, our analysis would remain valid in case of a finite grid along z. In this section, we consider a single staggered Yee grid. We slightly abuse notations used earlier and introduce the grid with primary nodes $x_{1-k},\dots,x_{k+1}$, and dual ones $\hat{x}_{1-k},\dots,\hat{x}_k$ on $(-\infty,+\infty)$ such that $x_i<\hat{x}_i<x_{i+1}<\hat{x}_{i+1}$ and $x_1=0$. The solution is defined at the primary nodes, its first derivative is at the dual ones. Primary and dual nodes correspond, respectively, to even and odd nodes of Lebedev's grid introduced earlier. We set $x_1=0$ and require the grid to be symmetric with respect to $x=0$.

We approximate equation (11) on this grid as

$$\begin{aligned}-\frac{\partial^2 w_i(z)}{\partial z^2}-\frac{1}{\hat{h}_i}\left[\frac{w_{i+1}(z)-w_i(z)}{h_i}-\frac{w_i(z)-w_{i-1}(z)}{h_{i-1}}\right]&\\ =2\frac{d\delta(z)}{dz}\frac{\delta_1^i}{\hat{h}_1}, \qquad i=2-k,\dots,k,&\\ w_i|_{z=\pm\infty}=0,\quad w_{1-k}(z)=0,\ w_{k+1}(z)=0,&\end{aligned} \tag{12}$$

where $h_i=x_{i+1}-x_i$, $\hat{h}_i=\hat{x}_{i+1}-\hat{x}_i$ and δ_1^i is the Kronecker function (i.e., $\delta_1^i=1$ if $i=1$, and $\delta_1^i=0$ otherwise).

With the help of the Fourier transform

$$F\cdot=\frac{1}{\mathrm{i}\sqrt{\lambda}}\int_{-\infty}^{\infty}e^{-\mathrm{i}\sqrt{\lambda}z}\cdot dz, \tag{13}$$

equations (11) and (12) can be presented, respectively, for $u(x,\lambda)=F\cdot w(x,z)$ as

$$\lambda u-\frac{d^2u}{dx^2}=2\delta(x),\quad u|_{x=\pm\infty}=0, \tag{14}$$

and for $W_i(\lambda)=F\cdot w_i(z)$ as

$$\begin{aligned}\lambda W_i-\frac{1}{\hat{h}_i}\left[\frac{W_{i+1}-W_i}{h_i}-\frac{W_i-W_{i-1}}{h_{i-1}}\right]=2\frac{\delta_1^i}{\hat{h}_1},&\\ i=2-k,\dots,k,\quad W_{1-k}=0,\ W_{k+1}=0.&\end{aligned} \tag{15}$$

Due to the symmetry with respect to the origin, equation (14) can be equivalently written on $[0,\infty)$ as

$$\lambda u-\frac{d^2u}{dx^2}=0,\quad \left.\frac{du}{dx}\right|_{x=0}=-1,\quad u|_{x=+\infty}=0. \tag{16}$$

We are interested in

$$f(\lambda)=u(0,\lambda)=-u(0,\lambda)\Big/\left.\frac{du(x,\lambda)}{dx}\right|_{x=0}, \tag{17}$$

where $f(\lambda)$ is commonly called the impedance function. Solving equation (16) analytically, we obtain $f(\lambda)=\lambda^{-1/2}$.

Now let us also reduce equation (15) to an equivalent boundary problem on $[0,\infty)$. For that purpose, we use only the nodes with positive indices from those defined earlier on $(-\infty,\infty)$. In addition, we need to introduce fictitious nodes $\hat{x}_0=0$ and some $x_0<0$ for imposing the discrete Neumann boundary condition precisely at the boundary $x=0$, so the new step $\hat{h}_1$ will be half of the old one, and the new step h_0 will be an arbitrary positive number. The system (15) can be equivalently reduced to

$$\lambda W_i-\frac{1}{\hat{h}_i}\left[\frac{W_{i+1}-W_i}{h_i}-\frac{W_i-W_{i-1}}{h_{i-1}}\right]=0,\quad i=1,\dots,k, \tag{18}$$

and boundary conditions

$$\frac{W_1-W_0}{h_0}=-1,\quad W_{k+1}=0. \tag{19}$$

The accuracy of the solution of equation (12) at $x=0$ is determined by the accuracy of W at the first node. The crucial fact is that $W_1(\lambda)=f_k(\lambda)$, where $f_k(\lambda)$ is a rational function of λ. It can be found from equations (18)–(19) by the simple Gauss

elimination, in the form of a Stieltjes continued fraction:

$$f_k(\lambda) = \cfrac{1}{\hat{h}_1\lambda + \cfrac{1}{h_1 + \cfrac{1}{\hat{h}_2\lambda + \ldots \cfrac{1}{h_{k-1} + \cfrac{1}{\hat{h}_k\lambda + \cfrac{1}{h_k}}}}}}. \quad (20)$$

The Stieltjes continued fraction (S-fraction) is an extremely well-studied tool used in many areas of pure and applied mathematics, such as theory of orthogonal polynomials, dynamical systems, Gaussian processes, number and approximation theories, etc. (Baker and Graves-Morris, 1996).

We want to optimize the grid with respect to the FD error of the Dirichlet data at the boundary W_1, that is,

$$\delta_k = |W_1(\lambda) - u(0,\lambda)| = |f_k(\lambda) - \lambda^{-1/2}|. \quad (21)$$

Thus, the problem of the grid optimization can be reduced to the problem of the Stieltjes rational approximation of the inverse square root. Several ways to construct such an approximant are described by Druskin and Knizhnerman (1999, 2000) and Ingerman et al. (2000). It is proven there that it is possible to construct the approximant converging exponentially as k increases.

Here, we present so-called "optimal geometric grids" according to Ingerman et al. (2000). It is known that, for the standard equidistant grids, the FD error is controlled by the grid step h [$O(h^2)$ for the Yee grid] and the distance to the boundary of the computational domain. The optimal geometric grid is a nonuniform grid which provides the maximally possible progression coefficient not increasing the approximation error.

Let us consider the n-point equidistant grid

$$h_i = h, \quad i = 1, \ldots, n,$$
$$\hat{h}_1 = h/2, \quad \hat{h}_i = h, \quad i = 2, \ldots, n.$$

Let us also construct the geometric progression grid

$$h_i = h\alpha^{i-1}, \quad i = 1, \ldots, k,$$
$$\hat{h}_1 = h/(1+\sqrt{\alpha}), \quad \hat{h}_i = h_i/\sqrt{\alpha}, \quad i = 2, \ldots, k,$$

such that $x_{k+1} = nh$. If α satisfies

$$\alpha = \exp\left(\gamma\pi/\sqrt{k}\right), \quad 0 \le \gamma \le 1, \quad (22)$$

then δ_k will be of the same order as the error of the n-point equidistant grid. Obviously, $\gamma = 1$ is optimal; it minimizes k for given h and n. So, for the same accuracy of the optimal and equidistant grids, we obtain

$$k \approx (\log n/\pi)^2.$$

Geometric grids are widely used for the FD approximations of singular solutions. However, the conventional approach optimizes the global truncation error. This approach implies centered differences with $\hat{x}_i = (x_{i-1} + x_i)/2$ and rather small progression coefficients for the grid steps, typically not exceeding 2.

Superconvergence of Lebedev's grid

Here, we explain the error cancellation phenomenon of the Lebedev grid outlined in a previous section (see Figures 2–3).

First, note that on every face of the grid domain Ω, two clusters satisfy the electric boundary condition (6), whereas the other two satisfy the magnetic condition (6). If we consider a Green's function in homogenous medium, then the effect of the boundaries can be estimated using the method of the fictitious images. Because of the two different types of boundary conditions, the first mirror reflection has different signs on the various clusters, so that after averaging the solutions, these reflections cancel. In other words, if the error of truncating the domain is positive for two clusters, it is negative for two other ones. So, Lebedev's grid effectively decreases the error of truncating the computational domain. This phenomenon is presented in Figure 3.

Let us now rigorously explain the error cancellation in the vicinity of the source shown in Figure 2. We derive a relationship between errors obtained on the different clusters (for constant coefficients). Based on this relationship, we show that, compared to a single cluster (Yee grid), the Lebedev grid cancels the error (up to a quadratic term) on the borehole axis.

Using the same assumptions and reasoning as in the previous subsection, the FD problem can be reduced to the approximation of the impedance function $f(\lambda) = \lambda^{-1/2}$ for equation (16). The 1D Lebedev scheme is reduced to two clusters, i.e., equation (18) and the dual scheme. To define this scheme, we add a fictitious node $\hat{x}_{k+1} > x_{k+1}$, remove the fictitious node x_0, and introduce variable V_i defined at dual nodes. New variables satisfy the dual equation

$$\lambda V_i - \frac{1}{h_i}\left[\frac{V_{i+1} - V_i}{\hat{h}_{i+1}} - \frac{V_i - V_{i-1}}{\hat{h}_i}\right] = 0, \quad i = 1, \ldots, k. \quad (23)$$

and boundary conditions

$$\frac{V_1 - V_0}{\hat{h}_1} = -1, \quad \frac{V_{k+1} - V_k}{\hat{h}_{k+1}} = 0. \quad (24)$$

Now, let us return to the averaging procedure for Lebedev's grid described earlier. Obviously, the sources for the both clusters satisfy condition (1) (see subsection "Averaging of sources, solutions, and error cancellation"). Condition (2) means that the center of the mass of the sources at every cluster should be located at $x = 0$. For the first cluster, this solution is satisfied automatically because the source is located at $x_1 = 0$ in equation (15). Now, let us consider the dual cluster. System (23)–(24) can be symmetrically extended to $(-\infty, \infty)$, so it will be the dual counterpart of equation (15) with the discrete sources located at $\hat{x}_1$ and the symmetric node. Obviously, V_0 defined at the fictitious node $\hat{x}_0$ is the solution on the dual cluster, interpolated at $x = 0$. So the 1D projection of the averaging procedure for the Lebedev grid described earlier would yield

$$u|_{x=0} \approx (W_1 + V_0)/2.$$

Let us estimate the error of the above approximation.

One can check, by direct substitution, that W and V satisfy the first-order system

$$c\sqrt{\lambda}W_j = \frac{V_j - V_{j-1}}{\hat{h}_j}, \quad j = 1, \ldots, k+1$$
$$c^{-1}\sqrt{\lambda}V_j = \frac{W_{j+1} - W_j}{h_j}, \quad j = 0, \ldots, k \qquad (25)$$

with some constant $c \neq 0$. For example, equation (18) can be obtained by excluding V from system (25) (for any nontrivial c), and similarly, by excluding W from system (25) one can obtain equation (23). Thus, with a proper choice of c, system (25) maps equation (18) into equation (23) and vice versa.

Now, multiplying the first equation of system (25) for $j = 1$ by the second one for $j = 0$, dividing the obtained equality by λ, and using the first boundary conditions (19) and (24), we obtain the equality

$$W_1 V_0 = \lambda^{-1} \frac{W_1 - W_0}{h_0} \cdot \frac{V_1 - V_0}{\hat{h}_1} = 1/\lambda. \qquad (26)$$

Recall that $u(0) = f(\lambda) = \lambda^{-1/2}$. Let δ_k be the impedance errors of the primary cluster, i.e.,

$$\delta_k = u(0) - W_1 = \lambda^{-1/2} - W_1.$$

Then using equation (26), we obtain

$$\begin{aligned}(W_1 + V_0)/2 &= \frac{1}{2}\left(W_1 + \frac{1}{\lambda W_1}\right) \\ &= \frac{1}{2}\left(\lambda^{-1/2} - \delta_k + \frac{1}{\lambda(\lambda^{-1/2} - \delta_k)}\right) \\ &= \lambda^{-1/2} + \frac{{\delta_k}^2}{2(\lambda^{-1/2} - \delta_k)}.\end{aligned}$$

For large k, the primary cluster error δ_k becomes small, so the total error of Lebedev's grid will be close to

$$\frac{1}{2}\lambda^{1/2}{\delta_k}^2.$$

The most important feature in the above definition of Lebedev's scheme is that the solutions W_1 and V_0 for both clusters are located at the same point $x = 0$. As a result, the total Lebedev error is squared. Even in the case of an equidistant grid, we obtain fourth-order convergence instead of second order. For the optimal grid, we double the exponential convergence rate.

Extension to induction problems with variable coefficients

A useful property of the optimal grids is that the one optimal for the Laplace equation can be optimal or nearly optimal for many other partial differential equations (PDEs) or systems including equation (5) with variable coefficients.

Let us, instead of equation (11), consider 2D scalar E-polarization problem in diffusion approximation

$$-\frac{\partial^2 w(x,z)}{\partial z^2} - \frac{\partial^2 w(x,z)}{\partial x^2} + \mathrm{i}b(x,z)w(x,z) = 2\delta(x)\delta(z), \qquad (27)$$

where $b = \omega\sigma\mu$ is a bounded real positive function.

First, we consider the case of constant b. Applying the same FD approach and the Fourier transform analysis, we can obtain the exact counterparts of all continuous and discrete equations of the previous subsections but with $\lambda + \mathrm{i}b$ instead of λ. So, the FD error will be given by

$$\| f_k(z) - z^{-1/2} \|$$

for Yee grid or its square for Lebedev's grid, with $z = \lambda + \mathrm{i}b$, and instead of the real approximation problem we arrive at the approximation at the complex plane. It is known that if a Stietltjes rational approximant exponentially converges on the real positive semi-axis, then it also exponentially converges on the complex plane, except for the real negative semi-axis (Baker and Graves-Morris, 1996, chapter 6). From this analysis made in the process of the proof of lemma 4.3 by Ingerman et al. (2000), it follows that for the complex approximation with $\mathrm{Re}(z) \geq 0$, the condition for γ in equation (22) should be replaced by

$$0 \leq \gamma \leq 1/\sqrt{2}.$$

From the above condition, the optimal progression is given by

$$\gamma = 1/\sqrt{2}.$$

We refer to this progression as to the "optimal geometric grid."

Let us now consider horizontally layered media, i.e., when $b = b(z)$. For this case, instead of the Fourier transform (3), one can use transform

$$F_b \cdot = \int_{-\infty}^{\infty} q(z,\lambda) \cdot dz,$$

where $-\lambda$ and $q(z,\lambda)$ are, respectively, eigenvalue and eigenfunction of operator

$$-\frac{d^2}{dz^2} + \mathrm{i}b(z)I,$$

i.e., $q(z,\lambda)$ is a uniformly bounded solution of equation

$$-\frac{d^2 q}{dz^2} + \mathrm{i}b(z)q = \lambda q$$

on $(-\infty, \infty)$. It is easy to see that F_b would allow us to treat the case of $b(z)$ the same way as the case with constant b.

Finally, let us discuss the most general case, when $b = b(x,z)$. For this case, we can use the asymptotic analysis of Borcea and Druskin (2002). Although that paper only considered in detail PDEs with coefficients depending on x, it was noted there that the asymptotic result for the forward problem can be straightforwardly extended to the case of $b = b(x,z)$. That result is formulated for the high-frequency asymptotics of the Fourier transform (13) of the solution, i.e., when $\lambda \gg b$. The result states that the error of the Fourier transform at $x = 0$ on the optimal grid can be estimated as

$$O(E_0(0)) + O\left(\frac{\|E_0\|_1 + \|E_b\|_1}{\sqrt{\lambda}}\right), \qquad (28)$$

where $E_0(0)$ is the error of the optimal grid for the homogeneous medium at $x = 0$, $\|E_0\|_1$ and $\|E_b\|_1$ are the L_1 global errors in the homogeneous medium and for $b(x,z)$, respectively. The proof is based on the fact that the variable coefficient does not affect the leading term of the PDE. The estimate (28) shows that for large λ, the dominant part of the error is defined by the error in the homogeneous medium. The latter converges exponentially thanks to the optimal grid. It is well known that the most difficult case for the conventional FD schemes is the

case of rapidly varying oscillatory components of the solution but, according to equation (28), for those, the optimal grid is almost as accurate as the optimal grid in the homogeneous medium. That means that fast convergence will be observed until the break-even point between first and seconds term of equation (28). After the first term becomes small, the convergence speed will be the same as the standard FD scheme for smooth solutions.

The 3D problem can be analyzed similarly, using 2D Fourier transform.

The final conclusion is that the superconvergent properties of the optimal and Lebedev grids remain valid for the induction problems with the skin depths significantly larger than the minimal steps of the FD grid. This assumption is always true for conventional induction logging problems; however, it may not hold for some other electromagnetic problems (for example, for magnetotellurics). We believe that for these problems the optimal grid approach still can be applied within a domain decomposition framework similar to the one presented in Asvadurov et al. (2000, 2002) for even more difficult time-domain acoustic logging problems in elastic media. However, the description of that approach is beyond the scope of this paper.

Implementation for the Lebedev FD scheme

Let us consider, as an example, the magnetic field of a magnetic dipole which is situated on the axis of a borehole crossing inclined anisotropic layers. We want to compute the magnetic field along this axis, having the exciting currents on the same axis. For gridding, we apply the approach of the previous section.

Let the borehole axis be the line $x = 0, y = 0$. Then, the optimal grids can be applied along x and y coordinates. We typically use the same grids along x and y. Let us, for example, consider the x grid. It consists of the primary and dual nodes of the optimal grid, symmetrically reflected with respect to the origin (with nodes $\hat{x}_0$ and x_0 excluded), so $M_x = 4k$ [see equation (2) and the previous section for the definitions]. Thus, in every half-space, we obtain the primary and dual optimal clusters, as in the previous section.

Before we defined only the progression factor $\exp(\pi/\sqrt{2k})$ for the optimal geometric grid. However, for the complete grid description, we need to define the minimal step and the boundary of the computational domain. As was mentioned earlier, the optimal geometric grid provides the same accuracy as the equidistant grid with the grid steps equal to the minimal step of the optimal grid and the same boundary of the computational domain. So for the choice of these two parameters, one can use the ad hoc rules adopted for conventional FD techniques. Those rules, however, can be significantly relaxed due to the error cancellation phenomena of Lebedev's scheme, described earlier.

NUMERICAL EXPERIMENTS

The efficacy of the developed scheme was illustrated in the benchmark comparison with the analytic solution for the dc electric potential in the presence of thin resistive fracture (Moskow et al., 1999), in which case the solution jumps across the fracture.

There were also several good benchmarks to check the presently described FD scheme against analytic solutions for layered media for induction logging applications (Anderson et al., 1999, 2001).

A comparison of our results with two independently derived solutions is presented in Figure 4. We examined the magnetic field of an axial 160-kHz transmitter along the axis of a conductive borehole intersecting a dipping anisotropic space. One can see that all three solutions are close to each other. Our results are in excellent agreement with those by Weiss and Newman (2002) for the imaginary part of the magnetic field and with those by Avdeev et al. (2002) for its real part.

Another comparison (Figure 5) shows the computed response of synthetic (skin-effect-corrected) induction logs for a 2C-40 sonde (one receiver coil is coaxial with a 20-kHz transmitting coil, offset by 1.016 m) traversing the crossbedded contact between an isotropic upper half-space and an anisotropic lower half-space. We use optimal x and y grids, whereas along the z-axis we set the grid to be equidistant between the transmitter and the receiver, and optimal geometric otherwise. We present the comparison with a quasi-analytical solution by Anderson et al. (2001). Note that the same example was considered by Weiss and Newman (2002), where they needed a grid of $59 \times 59 \times 59 = 205\,379$ nodes to obtain reasonable results, whereas the grids of $30 \times 30 \times 30 = 27\,000$ and $38 \times 38 \times 30 = 43\,320$ nodes were certainly not good enough. It is easy to see that our approach makes it possible to get reasonable results even for the grid of $12 \times 12 \times 28/2 = 2016$ nodes (that is, only three optimal steps along the x- and y-directions to the right and to the left from the origin). Both primary and dual nodes are counted here. By the division by two we mean that only the nodes of the subgrid R are used for the FD approximation in equation (5), rather than all nodes (see Figure 1). The results for the grids of $16 \times 16 \times 46/2 = 5888$ and $20 \times 20 \times 46/2 = 9200$ nodes are hardly distinguishable from the analytical solution. We should point out that the FD stencil in our scheme is even slightly smaller than that in Weiss and Newman (2002). This means an acceleration at least of 20–40 times, provided that the same linear solver is used.

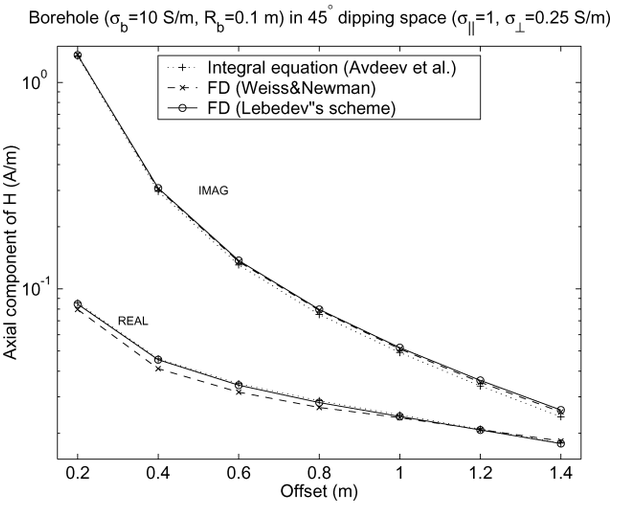

FIG. 4. Comparison of the results for the axial magnetic field with the results of two other numerical 3D codes in presence of a borehole. The quantity plotted is the difference between the total field and the field from an equivalent source located in a vacuum.

Let us consider self-consistency convergence tests for more complicated 3D models. We calculated the magnetic induction along the axis of a borehole with an invasion intersecting two dipping layers, one of which is anisotropic (see Figure 6). A 52.65-kHz transmitting coil is oriented along the x-axis and placed at the origin. Figure 7 shows the plots of the $\mathrm{Im}B_{xx}$ and $\mathrm{Im}B_{xz}$, two components of the magnetic induction versus z. Along the x- and y-directions, the geometrically optimal grid is used, with different numbers of steps k. We solve the problem on the whole axis x and on the positive semi-axis y using the symmetry of the model with respect to the plane $y=0$. This means that $M_x=4k$, whereas $M_y=2k$ [see equation (2) for the definition of M_x and M_y]. A detailed-enough, nonoptimal grid along the z-axis, with number of nodes $M_z=98$, is used in all the comparisons.

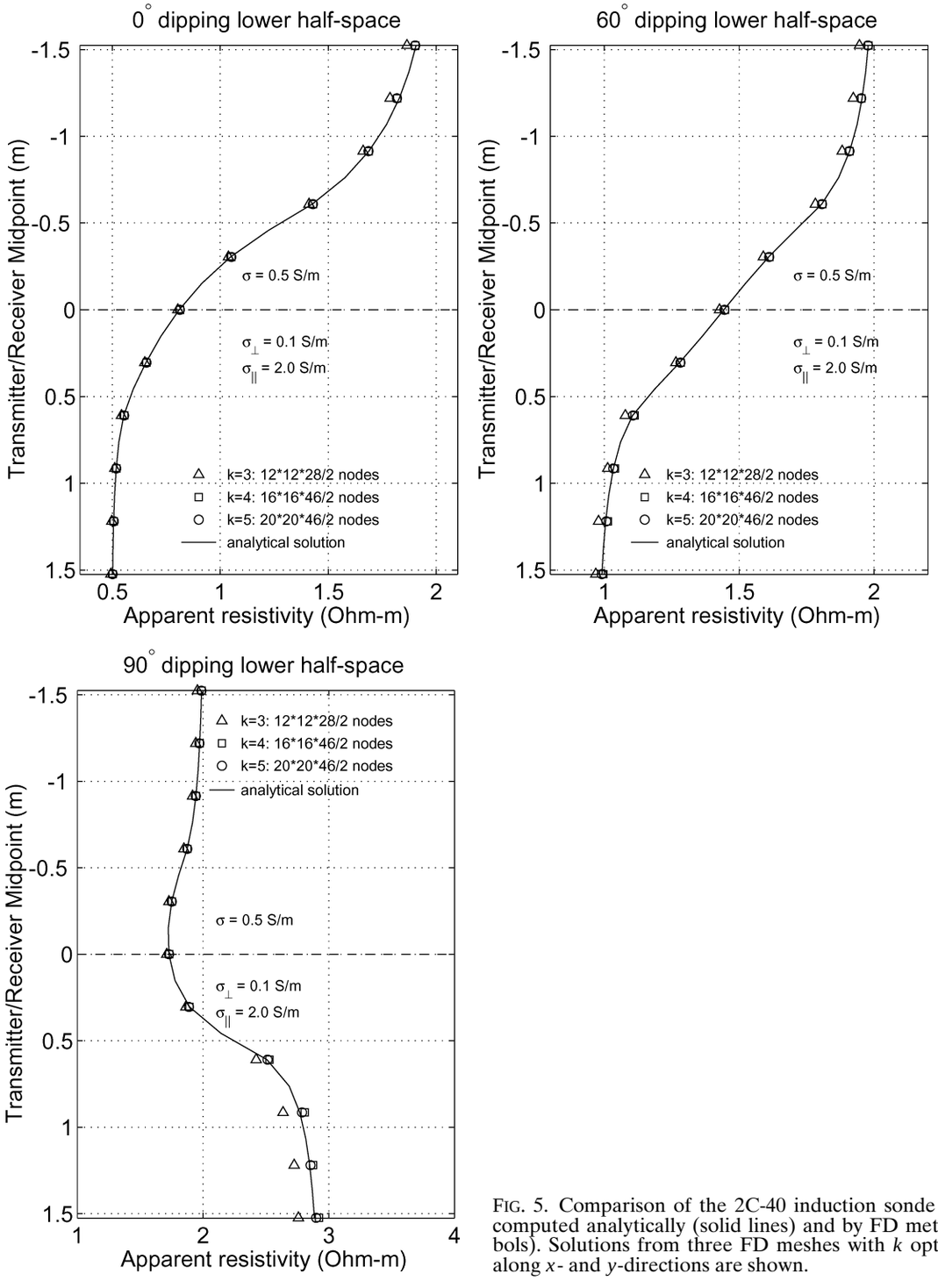

FIG. 5. Comparison of the 2C-40 induction sonde responses computed analytically (solid lines) and by FD method (symbols). Solutions from three FD meshes with k optimal steps along x- and y-directions are shown.

Figure 7 shows that the plots for the optimal grids with $k=4$, $k=5$, and $k=6$ are practically identical. Moreover, even the plots with $k=3$ are almost as good, except for a few nodes near the transmitter.

Let us note that in a homogeneous medium, B_{xz} would be equal to zero, so we can observe the pure effect of inhomogeneity. The convergence of the solution, as k increases, is as fast as for the case of B_{xx}.

In Figure 9, we plot the axial component of the magnetic induction ($\mathrm{Im}\,B_z$) along the axis of the borehole intersecting a dipping thin anisitropic layer, whose conductivity in perpendicular direction σ_N is of high contrast with respect to the background conductivity. The model is depicted in Figure 8. A 52.65-kHz transmitting coil is oriented along z-axis and placed at the origin. The upper plot in Figure 9 illustrates the case when σ_N is equal to the background conductivity, whereas for the lower plot it is 200 times smaller. It is easy to see that, in both cases, the plots of $\mathrm{Im}\,B_z$ for the grids with the number of optimal nodes $k=6$ and $k=12$ can hardly be distinguished. This is despite the fact that the width of the anisotropic layer (0.25 m)

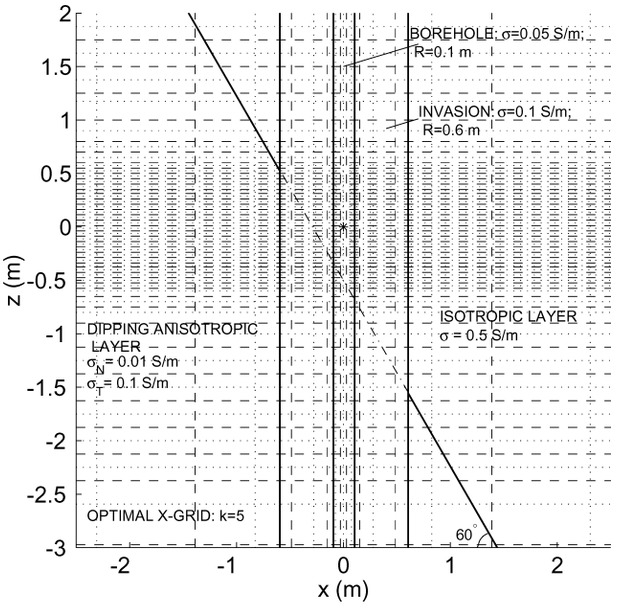

FIG. 6. A model of the medium on the background of Lebedev's grid containing 98 z-nodes and $4k$ optimal x-nodes. Dotted lines show the basic grid, whereas dashed lines show the dual grid. The asterisk signifies the position of the transmitter.

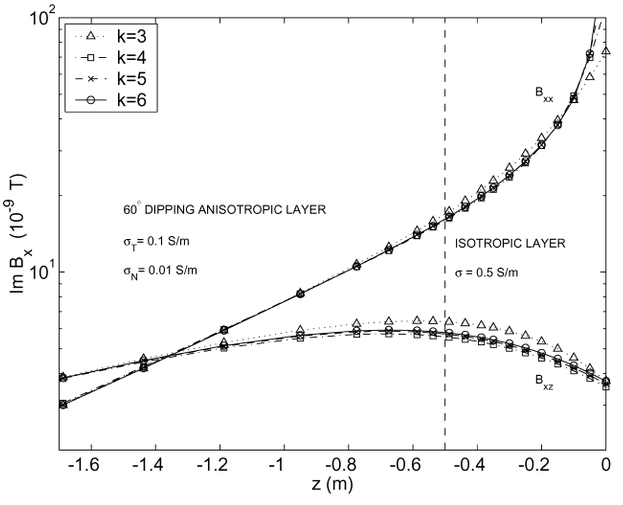

FIG. 7. The imaginary part of the horizontal ($\mathrm{Im}\,B_{xx}$) and vertical ($\mathrm{Im}\,B_{xz}$) magnetic induction versus z for the model containing two inclined layers, a borehole, and an invasion (see Figure 6).

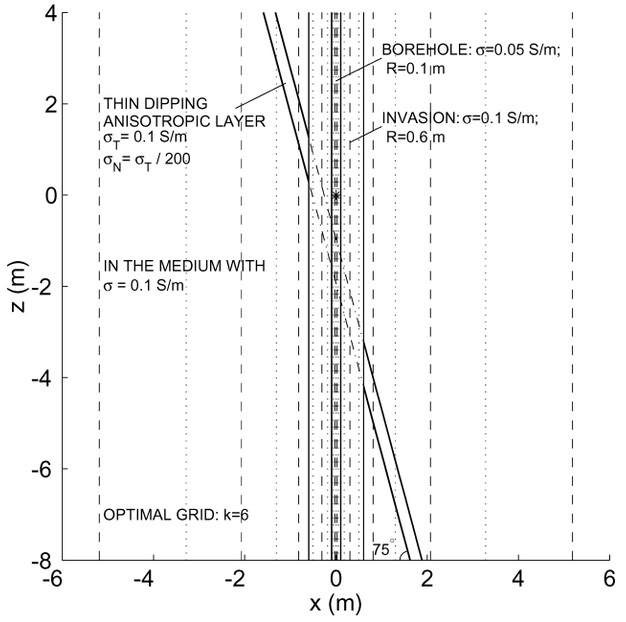

FIG. 8. A model containing a thin inclined layer with the perpendicular conductivity of high contrast. The optimal grid along x for $k=6$ (i.e., 24 nodes) is depicted as vertical dotted lines (the basic grid) and dashed lines (the dual grid). The grid along z is not depicted, since it is the same as for the previous model (see Figure 6).

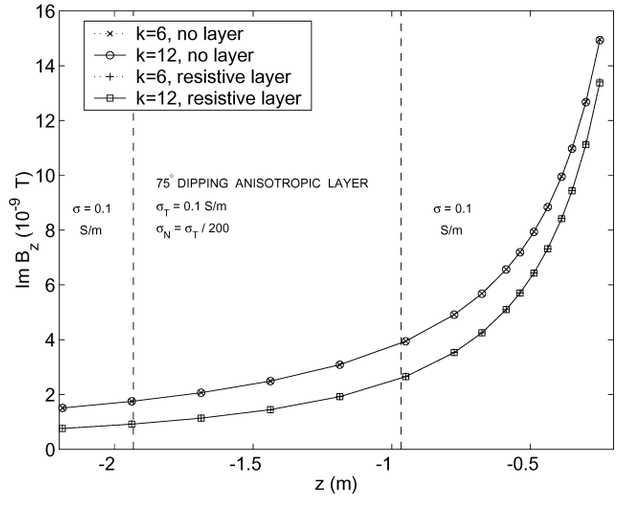

FIG. 9. The imaginary part of the vertical magnetic induction $\mathrm{Im}\,B_z$ versus z for the model containing a thin dipping anisotropic layer of high contrast (see Figure 8).

is less than the steps of the optimal grid for $k = 6$ along the x- and y-directions (the optimal x-grid is depicted in Figure 8 as a background).

For all the considered examples, the computation time did not exceed 1 minute per model on a 1-GHz Pentium. Recently, we achieved further acceleration by implementing optimal grids also along the measurement line z and using a special postprocessing technique, as in Asvadurov et al. (2002). However, this approach is beyond of the scope of this paper.

CONCLUSIONS

The examined examples illustrate the high effectiveness of Lebedev's staggered grid for computing electromagnetic fields in 3D inhomogeneous anisotropic media for induction logging applications. The proper averaging of the parameters of the medium and the optimal grid approach make it possible to handle models of finely layered media with high contrast in conductivity, using the FD grids containing only a few nodes along the x- and y-directions. This means that the new FD scheme allows handling complicated 3D models more than one order faster than other known FD schemes and, therefore, can be successfully used for the interpretation of induction log data in fully anisotropic formations.

ACKNOWLEDGMENTS

We are indebted to our friends and colleagues Barbara Anderson, Leonid Knizhnerman, David Ingerman, Shari Moskow, Sergey Asvadurov, Dzevat Omeragic, Liliana Borcea, and Ping Lee for useful discussions and valuable help in different stages of this work. Extensive editing by Mark Everett and two anonymous referees significantly improved the quality of the manuscript.

REFERENCES

Anderson, B., Barber, T., and Gianzero, S., 2001, The effect of cross-bedding anisotropy on induction tool responce: Petrophysics, **42**, 137–149.

Anderson, B., Druskin, V., Lee, P., Dussan, E., Knizhnerman, L., and Davydycheva, S., 1999, The response of multiarray induction tools in highly dipping formations with invasion and in arbitrary 3D geometries: The Log Analyst, **40**, 327–344.

Asvadurov, S., Druskin, V., and Knizhnerman, L., 2000, Application of the difference Gaussian rules to solution of hyperbolic problems: J. Comp. Phys., **158**, 116–135.

———2002, Application of the difference Gaussian rules to solution of hyperbolic problems II. Global expansion: J. Comp. Phys, **175**, 24–29.

Avdeev, D. B., Kuvshinov, A. V., Pankratov, O. V., and Newman, G. A., 2002, Three-dimensional induction logging problems, part I: An integral equation solution and model comparisons: Geophysics, **67**, 413–426.

Baker, G. and Graves-Morris, P., 1996, Padé approximants: Cambridge University Press.

Borcea, L., and Druskin, V., 2002, Optimal finite-difference grids for direct and inverse Sturm-Liouville problems: Inverse Problems, **18**, 979–1001.

Davydycheva, S., and Druskin, V., 1995, Staggered grid for Maxwell's equations in an arbitrary 3D in homogeneous anisotropic media, *in* Proc. Internat. Symp, on three-dimensional electromagnetics: Schlumberger-Doll Research, 181–187.

———1999, Staggered grid for Maxwell's equations in arbitrary 3D inhomogeneous anisotropic media, *in* Oristaglio, M. and Spies, B., Eds., three-dimensional Electromagnetics: Soc. Expl. Geophys., 138–145.

Druskin, V., and Knizhnerman, L., 1994, Spectral approach to solving three-dimensional Maxwell's equations in the time and frequency domains: Radio Science, **29**, 937–953.

Druskin, V., and Knizhnerman, L., 1999, Gaussian spectral rules for the three-point second differences: I. A two-point positive definite problem in a semi-infinite domain: SIAM J. Numer. Anal. **37**, 403–422.

———2000, Gaussian spectral rules for second order finite-differences schemes: J. Num. Alg. **25**, 139–159.

Druskin, V., Knizhnerman, L., and Lee, P., 1999, A new spectral Lanczos decomposition method for induction modeling in arbitrary 3D geometry: Geophysics, **64**, 701–706.

Habashy, T. M., Groom, R. W., and Spies, B. R., 1993, Beyond the Born and Rytov approximations: a nonlinear approach to electromagnetic scattering: J. Geophys. Res.—Solid Earth, **98**, B2, 1759–1775.

Igel, H., Mora, P., and Riollet, B., 1995, Anisotropic wave propagation through finite-difference grids: Geophysics, **60**, 1203–1216.

Ingerman, D., Druskin, V., and Knizhnerman, L., 2000, Optimal finite-difference grids and rational approximations of square root. I. Elliptic problems: Comm. Pure and Appl. Math., **53**, 1039–1066.

Lebedev, V. I., 1964, Difference analogies of orthogonal decompositions of basic differential operators and some boundary value problems. I: Soviet Comput. Maths. Math. Phys., **4**, 449–465 (in Russian).

Moskow, S., Druskin, V., Habashy, T., Lee, P., and Davydycheva, S., 1999, A finite difference scheme for elliptic equations with rough coefficients using a Cartesian grid nonconforming to interfaces: SIAM J. Numer. Anal. **36**, 442–464.

Wang, T., and Fang, S., 2001, 3D electromagnetic anisotropy modeling using finite differences: Geophysics, **66**, 1386–1398.

Weidelt, P., 1999, 3D conductivity models: Implications of electrical anisotropy, *in* Oristaglio, M. and Spies, B., Eds., Three-dimensional electromagnetics: Soc. Expl. Geophys., 119–137.

Weiss, C. J., and Newman, G. A., 2002, Electromagnetic induction in a fully 3D anisotropic earth: Geophysics, **67**, 1104–1114.

Yee, K. S., 1966, Numerical solution of initial boundary value problems involving Maxwell's equations in isotropic media: IEEE Trans. Ant. Prop., **AP-14**, 302–307.